WELL LOGGING

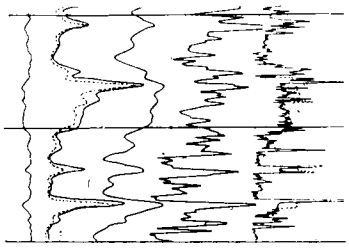

Determination of a More Accurate Porosity and Mineral Composition in Complex Lithologies with the Use Of the Sonic, Neutron and Density Surveys

WAYLAND C. SAVRE | GULF OIL CORP. ODESSA, TEX.

Abstract

The Permian system of West Texas contains large undifferentiated masses of carbonate rocks with admixtures of evaporites. These rocks exhibit markedly variable characteristics as observed with radioactivity, acoustic and electrical surveys.

All surveys used independently may present different porosity values as a result of mineralogical heterogeneity, inadequate information regarding pore geometry, or variance in residual oil.

The widespread, singular use of gamma ray-neutron surveys has resulted in general misconception regarding the occurrence of porosity and consequently various aspects of reservoir interpretation. Hydrogen bound by water of crystallization in gypsum produces high apparent porosities on the neutron survey. Only recently have analytical methods been employed which attempt to eliminate these effects in core analysis. Anhydrite and gypsum may produce porosity errors when average velocity or density information is used with the sonic or density logs.

With the development and improvement of logging tools provided by more sophisticated electronics and instrumentation, and the use of parameters which are a function of intrinsic rock properties, more accurate porosity determinations may be obtained.

The formation density log, the sonic log and the neutron log provide three independent measurements of physical properties of formations in situ. Usable relationships between these properties and porosity are well known. The inaccuracies of computing porosity from average matrix parameters (grain density, matrix velocity and neutron response) are minimized by considering the matrix parameters to be limited variables and making simultaneous solutions of three equations. This method of analysis permits determination of more accurate porosity values, and the percentage of each of three minerals comprising the rock matrix-dolomite or limestone, gypsum and anhydrite. In certain cases gas may be detected.

Production tests, known reservoir characteristics and core information point out interesting correlative and corroborative results.

Introduction

The Permian system of West Texas and adjacent areas contain large masses of carbonate rocks that often lack readily distinguishable correlative markers and that exhibit subtle diversity of mineralogy.

The neutron survey so widely used in these rocks, in past years, is subject to porosity error when gypsum is present. So also are the sonic and density logs which, in addition, are affected by anhydrite. Field use indicates that the three surveys may be used simultaneously to calculate a rock composition and to obtain a more accurate* value of porosity in formations comprised of dolomite or limestone, anhydrite, and gypsum, when the three major constituents are known.

Log analysis has been difficult in carbonate rocks. It has been complicated by uncertainties in porosity determination and has depended heavily upon "experience factors" in particular areas or fields. The problems of calculating true porosity result from the many variations in rock type, particularly with reference to pore geometry; the changes in matrix composition, which affect to some degree the response of all porosity devices now in use; and the effects of residual oil. The thin-bedded nature of many zones of interest further compounds the problem.

This paper will consider some of these problems in detail and present a solution which has seen practical use with satisfactory results in a large number of applications.

It may appear, to some readers, that an excessive amount of space has been devoted to a discussion of rock characteristics in a paper primarily concerned with introducing a method of log analysis. The writer feels that accurate log interpretation can only be accomplished with a sound general knowledge of the rocks in which the surveys are to be used.

General Lithologic Considerations

Permian carbonate rocks are particularly interesting in their diversity. Several thousand feet may be described comprehensively in a few broad generalizations, yet an accurate, short-interval study may require many paragraphs to adequately describe significant variations in lithology. The variations have a significant effect upon the choice of "tortuosity exponent"[1] selected for microsurvey

Original manuscript received in Society of Petroleum Engineers office May 24, 1963. Revised manuscript received Aug. 1, 1963.

*This value for ease of differentiation will be referred to as calculated true porosity, or at times true porosity.

[1]References given at end of paper.

work and may provide some insight regarding depth of invasion, or value of residual oil which must be considered.

These rocks are predominantly dolomite and limestone, fine to medium crystalline, well indurated, anhydritic and gypsiferous. They exhibit the gamut of porosity variation, including fracture, solution (often faunal derived) and intercrystalline varieties. Intergranular porosity is present in many of the oolite and coquinoid facies. The porosity is "effective" in so far that portions of the pore space have not been completely isolated by diagenetic processes, or by secondary distribution of evaporites. The porosity may, in many cases, include pore space which is wholly or almost entirely isolated, but may still contain hydrocarbons that may be recovered by modern treating methods. There are locally carbonaceous, silty, slightly argillaceous, and silicified carbonate facies. There are also associated siltstone and shale beds, the former often confusing interpretation. Although some clay minerals[2] may be present interstitially and occasionally as inclusions in the carbonate units, they do not appear to be generally present in troublesome quantities. X-ray diffraction analysis of random dolomite specimens from the San Andres and Clearfork have indicated only traces of clay minerals—in these instances, illite.

Gypsum and Anhydrite

It has become abundantly apparent from the study of cores, and electrical and neutron surveys, that well developed porosity and significant reservoir characteristics may show considerable change within short distances stratigraphically and geographically, because of a change in the quantity or the types of evaporites present. Fig. 1 illustrates this condition as observed by the neutron and salt mud electrical surveys before the innovation of the useful sonic and density logs. The variability of porosity and evaporites as observed in examples of San Andres lithology are shown in Fig. 2.

The specimens A through E are typical examples of San Andres dolomite lithology, grading from excellent porosity and permeability at A through lesser amounts until both are essentially lacking at E. Evaporites which are almost absent in A can be seen wholly or partially filling some pore space in B, and the majority of the visible solution porosity has been filled in the specimen at D. The gypsum shown at F occurs as a partial filling of a solution cavity from the Grayburg formation of West Texas.

A large amount of anhydrite and/or gypsum may occur as interstitial material and avoid detection by megascopic examination of well cuttings or cores. In some cases, however, the percentage may be great enough to impart a grey color to the rock, or constitute the entire matrix. In most instances some evaporites are visibly present as beds and nodules, or may occupy fractures and solution porosity as shown in Fig. 3.

The evaporite nodule in plug A is typical of the dense, blue-white, fine-crystalline "anhydrite" so often described in cores of Permian dolomite. Here, the chalk white part of the nodule indicates the effect of dehydration after being subjected to a high temperature, revealing that portion which was gypsum. The light grey interior of the nodule remains as anhydrite. In this instance the great majority of the material occupying the visible pore space in the rest of the plug was gypsum.

Plugs B and C show similar alteration. The fracture in plug C exhibits relict anhydrite as a narrow, broken, light-grey zone in the center of an altered gypsum "halo". Plug B indicates the porosity measured with a Boyle's law porosimeter before and after dehydrating the gypsum present. The porosity of 7.2 per cent measured after dehydration represents an increase of 553.8 per cent.

Gypsum is usually present as a peripheral development or "halo" in the dense nodular or "massive" accumulations and may comprise a small percentage of the whole. If the anhydrite itself exhibits fractures, gypsum may be present within the fractures as adjacent alteration or as fillings. Deposits in intercrystalline and solu-

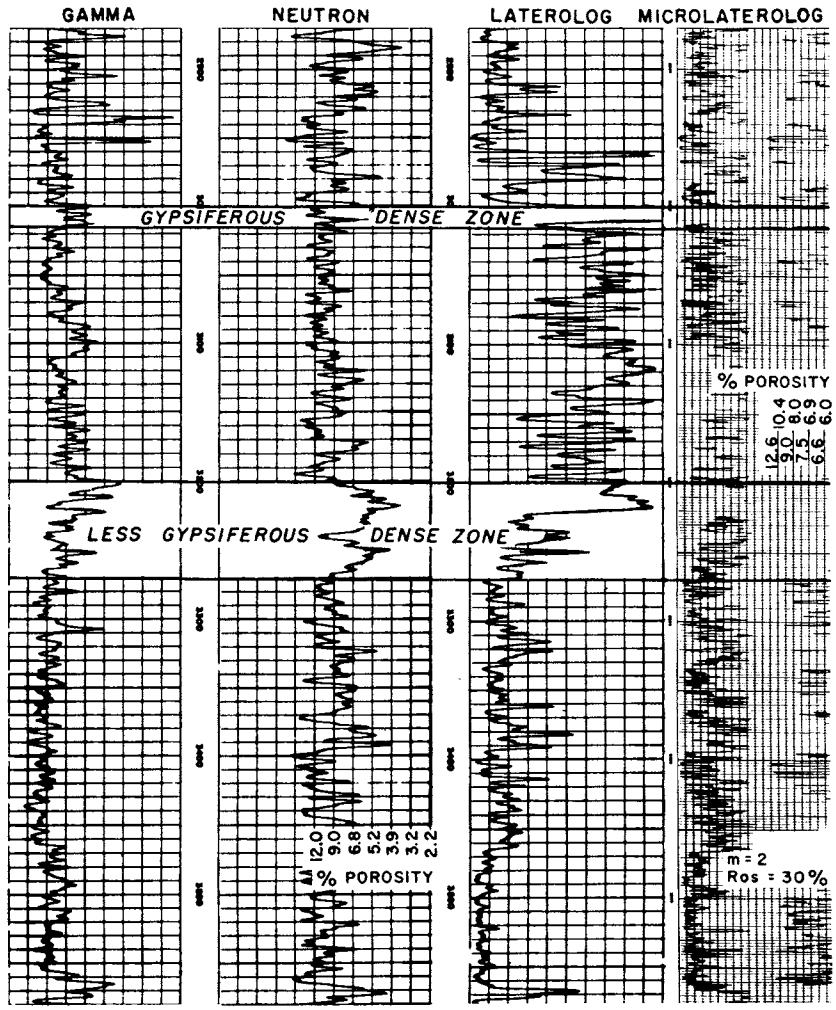

Fig. 1—The porosity surveys illustrated above (neutron and MicroLaterolog) show contrasting values throughout the logged interval. Note that the neutron log does not delineate the designated upper dense zone as the electrical surveys do. Relatively high porosities are indicated by the neutron survey because of the effects of the gypsum disseminated throughout the section. The Laterolog is included to show that the MicroLaterolog response is not a result of high residual oil saturation.

tion porosity, however, contribute larger percentages of gypsum, often with small amounts of anhydrite remaining as a relict mineral as shown in Fig. 4c.

The photomicrographs in Fig. 4c show both intercrystalline porosity and a small amount of solution porosity. This is quite aparent in plane polarized light with crossed nicols under the petrographic microscope, but in the illustrations cannot be distinguished from pores filled with gypsum at extinction.

Anhydrite, showing a peripheral alteration to gypsum, is in the center of the field in Fig. 4a. The anhydrite exhibits well developed cleavage and good relief under plane polarized light without crossed nicols in this example. Irregular grey areas below are gypsum with small angular remains of anhydrite which appear as inclusions. The matrix is comprised of fine crystalline dolomite.

The fusulinid mold shown in Fig. 4b contains gypsum, as does the fracture to the right. Very small amounts of relict anhydrite appear as somewhat angular and elongate particles

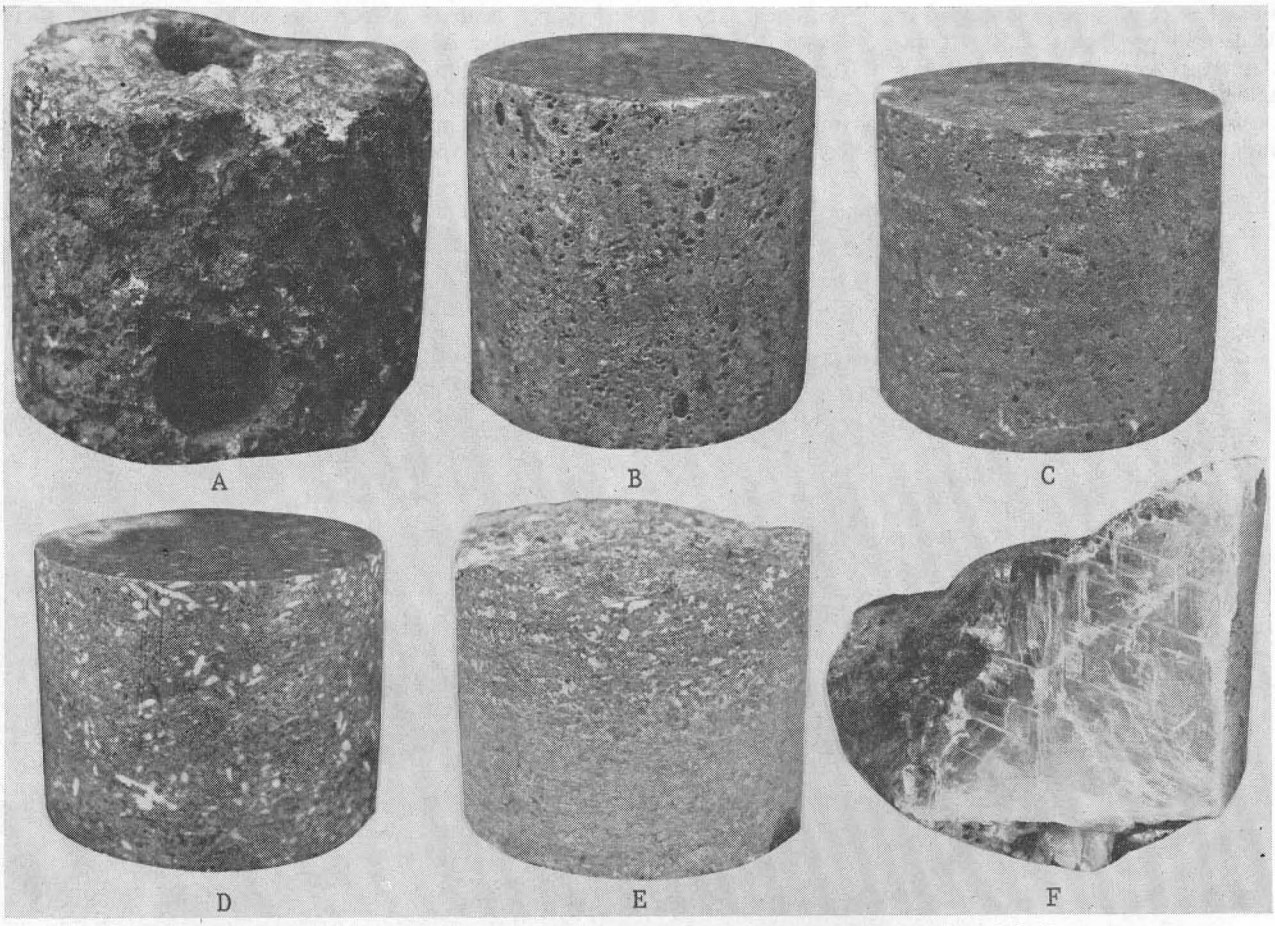

Fig. 2—Variability of porosity and evaporites in examples of San Andres lithology.

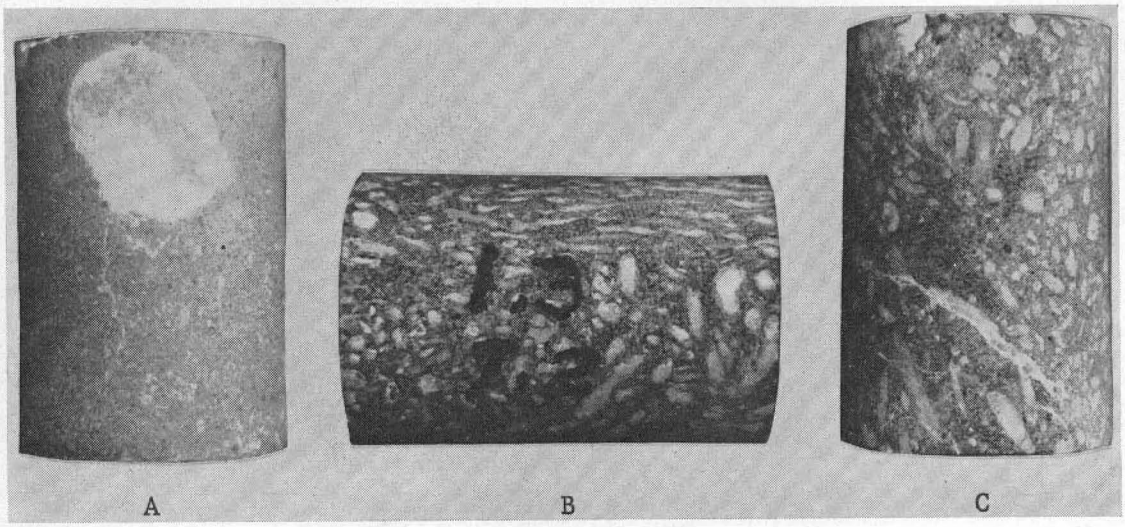

Fig. 3—Visible evaporites in well samples.

within the gypsum. Unfilled fusiform molds of this type are a common source of porosity in Permian carbonate rocks.

An irregular solution cavity and fracture filled with gypsum and anhydrite are shown in Fig. 4c. The anhydrite appears as the light grey, angular inclusions within the relatively clear gypsum-filled areas. The surrounding ground mass is dolomite.

Prior to the last three or four years gypsum has rarely been mentioned in rock descriptions below 2,500 ft unless it was observed as clear crystals of selenite. Almost without exception, the compact, vari-colored, micro-crystalline nodules and pore fillings observed have been reported as anhydrite. Interestingly this is approximately the same description applied to occurrences of gypsum by Goodman.[3] Conversely, some specimens identified by him in the field, and on macroscopic examination in the laboratory, as gypsum were identified with the microscope as anhydrite. Our own observations indicate both minerals are usually present with no obvious macroscopic differences in appearance. If a specimen is heated above 125 C for a short period of time the gypsum will be converted to a hemihydrate or anhydrite with immediately apparent changes in color and opacity, as previously shown in Fig. 3, while the anhydrite remains unaffected. Identification under the microscope, as shown in Fig. 4, shows the presence of gypsum and anhydrite in intercrystalline and solution pore space. It becomes evident that swift and reliable megascopic differentiation of these minerals, as they usually occur in the Permian carbonate rocks, is impossible, and more diagnostic determinative methods must be used to evaluate quantitatively their effect upon the various "porosity" surveys.

Core Analysis

The effect of gypsum on porosity measurements made by conventional

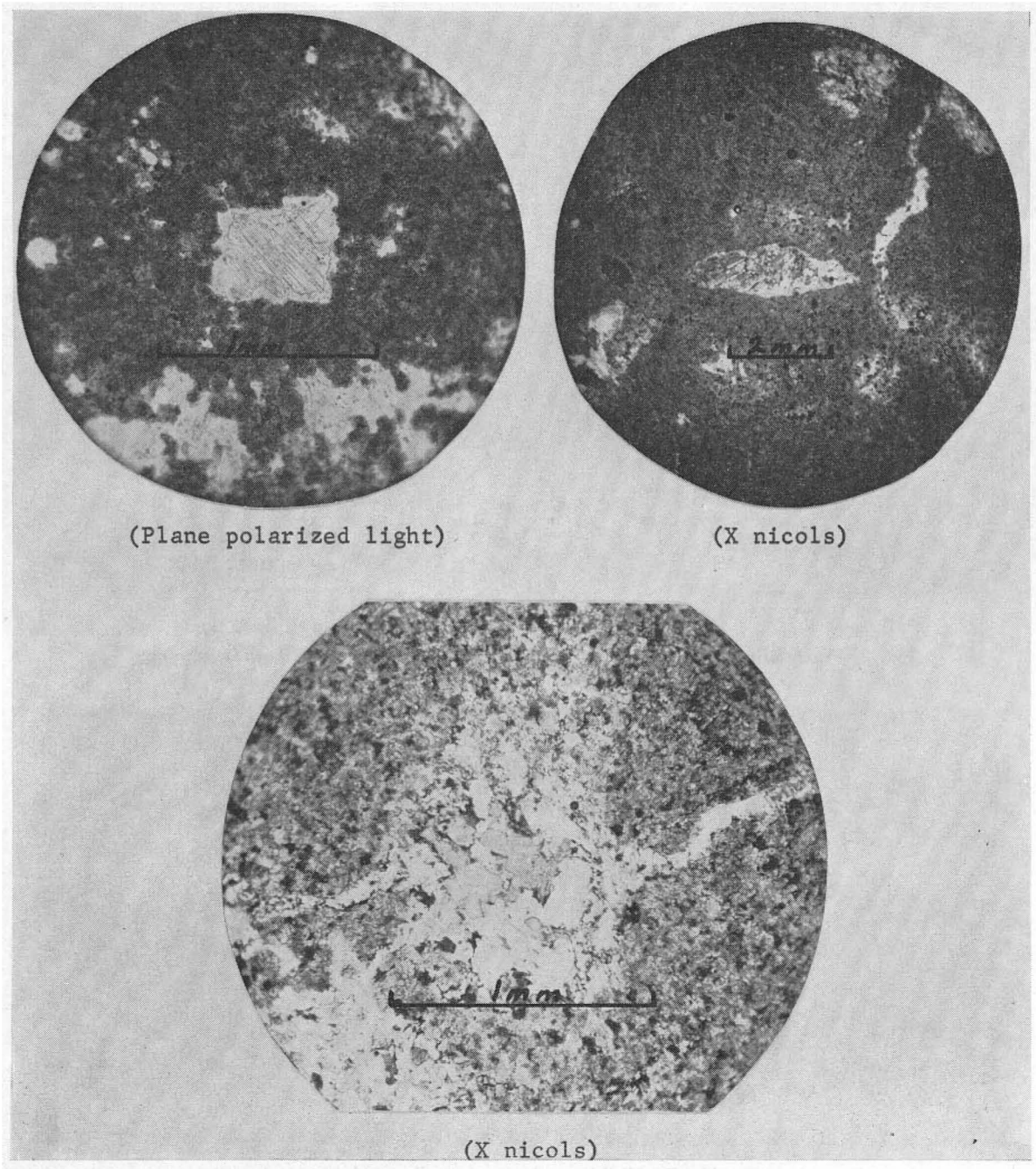

Fig. 4—Photomicrographs of intercrystalline and solution porosity.

core analysis has been discussed by Bynum and Koepf[4] and Hurd and Fitch.[5] They have shown that porosity error results when gypsum ($CaSO_4 \cdot 2H_2O$) is dehydrated prior to and during core analysis. The error may range from approximately 36 to 48.8 per cent of the volume of gypsum present, depending upon the type of extraction used or the method of measuring pore space. Recently employed analytical techniques which attempt to eliminate the effects of gypsum usually are conducted at temperatures below 60 C to prevent serious dehydration of the mineral. In routine analysis of this sort, practical problems of cleaning and drying rocks with low permeability, and the inability to obtain porosity and residual fluid data from the same sample, are encountered.

The Electric Logs

The MicroLaterolog may be used satisfactorily for porosity evaluation if adequate "tortuosity exponents" and values of residual oil saturation are known. Accurate information regarding the local variability of both is difficult, if not impossible, to obtain. However, resistivity changes reflecting residual oil saturation (or *Sxo*) make the MicroLaterolog a valuable tool in movable oil analysis.[6]

The Neutron Log

The neutron and gamma radiation surveys have been widely used in carbonate rocks, perhaps for reasons of economy more than any other. The neutron survey has also been most deceptive where minerals containing water of hydration are present. The neutron tool observes hydrogen contained in chemically bound water as well as that contained in pore space fluids. Gypsiferous rocks will consequently produce a neutron porosity which is higher than that which is actually present. This apparent porosity can be expressed by the equation

$$\phi_n = \phi + (1 - \phi)\,(0.49G). \quad (1)$$

where ϕ_n is the apparent neutron porosity, ϕ is true porosity and G is the percentage of gypsum in matrix.

As shown, the "pseudo" porosity contributed by gypsum will be 49 per cent of the total gypsum present, a considerable source of error in highly gypsiferous rocks. Because the presence of anhydrite and gypsum is often the reason for lack of porosity, it becomes apparent that a large percentage of porosity error may occur in the low-to-medium porosity ranges. The amount of error may not be of concern to some who may be interested in only the presence of porosity rather than in a specific value. It becomes significant however when reservoir boundaries appear porous, and considerable sums of money are spent in fruitless effort to stimulate impervious intervals to production. Before the sonic and density logs came into practical use, many instances of anomalous, high, neutron porosity were observed where electric logs were available for comparison. Such an instance in a San Andres horizon is shown in Fig. 5b. In comparison, the correlative but less gypsiferous interval from a nearby area is illustrated in Fig. 5a. The problem was apparent, but, until additional information could be obtained from sources other than electric logs, a solution was impossible. General acquaintance with comparisons of neutron-derived porosity and that from conventional core analysis makes inclusion of such data unnecessary here.

The Density Log

The density log, in measuring bulk density, reflects changes in rock composition, pore space and contained fluids. Accuracy in porosity determination cannot be obtained without accurate knowledge of the other variables. The true densities of most of the minerals with which we may be concerned are generally known. It has

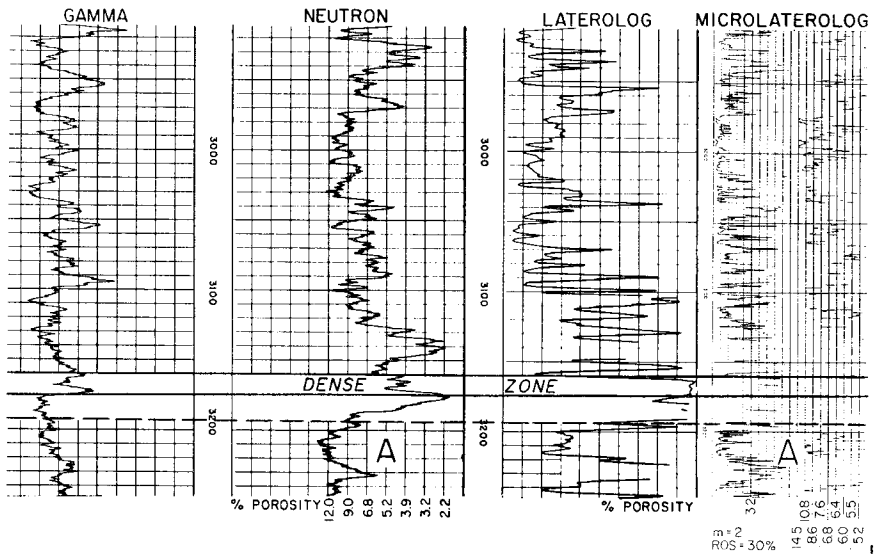

5a

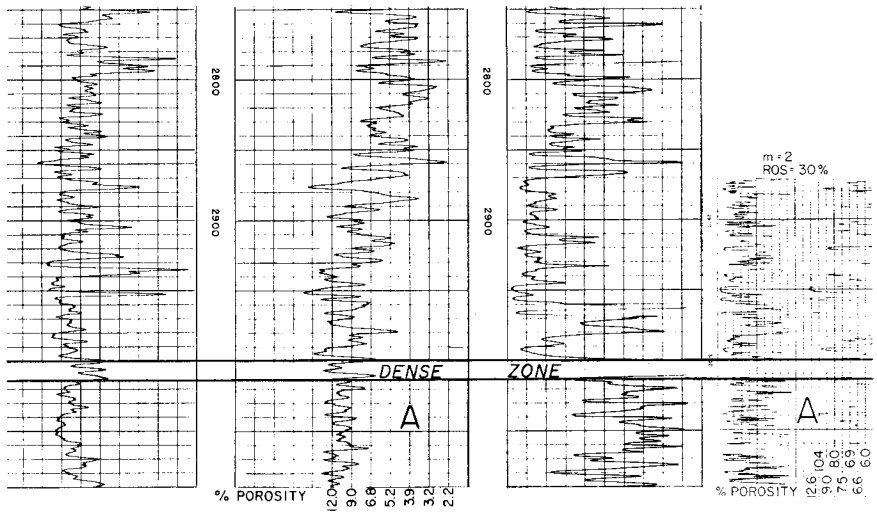

5b

Fig. 5—Figs. 5a and 5b contrast correlative horizons in the same field. The electric logs are in close agreement in the designated dense zone. The neutron surveys disagree in this and in other horizons. Fig. 5b indicates comparatively high neutron porosities as a result of the effects of gypsum. On the Micro-Laterolog surveys the porous zone, designated A, shows less porosity in Fig. 5b. The neutron survey, however, does not indicate the same relative change.

been indicated, however, that the density tool reflects electron density rather than true density. This is not serious in that the differences are small and corrections may be made if necessary.[7]

The density tool's response to porosity and matrix effects is shown by the equation:

$$\rho_b = \phi\,\rho_f + (1 - \phi)\,\rho_{g(ave)} \quad . \quad (2)$$

Where, in a formation comprised of dolomite, anhydrite, and gypsum

$$\rho_{g(ave)} = D\,\rho_{g(dol)} + A\,\rho_{g(anh)} + G\,\rho_{g(gyp)} \quad . \quad . \quad . \quad . \quad (3)$$

ρ_b = the bulk density of the formation

ρ_f = the fluid density

$\rho_{g(ave)}$ = the average grain density of rock matrix

$\rho_{g(gyp)}$ = 2.35 gm/cc, the density of gypsum

$\rho_{g(anh)}$ = 2.98 gm/cc, the density of anhydrite

$\rho_{g(dol)}$ = 2.82 gm/cc, the density of dolomite

ϕ = the percentage of porosity

D = the fraction of matrix that is dolomite

A = the fraction of matrix that is anhydrite

G = the fraction of matrix that is gypsum

and $D + A + G = 1$.

Where cuttings, cores, or other data indicate that limestone, rather than dolomite, is present, Eq. 3 is modified accordingly. The grain density for limestone is considered to be 2.71 gm/cc.

General use of the density log requires an average value for matrix density which may vary with the area or formation of interest. This is conventionally derived from a plot of log bulk densities and porosities measured by core analysis. Laboratory measurements of matrix densities are occasionally available, in which case averages of these values are often used in the immediate area.

In evaporitic carbonates, a massive section of anhydrite is readily recognized by a bulk density approaching or reaching 2.98 gm/cc. If, in such a zone, average matrix densities of dolomite were rigidly observed, a porosity less than zero would be computed. Thus, an anhydritic dolomite or limestone will exhibit a density-derived porosity lower than that actually present when the anhydrite is not properly taken into consideration. An opposite effect results when gypsum, with a low grain density of 2.35, is present; erroneously high values of porosity result. For example, gypsum, with zero porosity, exhibits the same density as a dolomite with 25.8 per cent porosity. Mixtures of anhydrite, gypsum, and dolomite or limestone present difficult interpretive problems unless the relative percentage of each may be determined.

The ability of the density log to detect gas in zones of shallow invasion where other porosity control is available is generally known. When used with the neutron only in evaporitic rocks, the effects of gypsum may nullify the neutron gas response, and anhydrite may affect the density log such that gas identification becomes very unreliable or impossible. It has been noted by the author that density log repeatability in a gas zone may be poor in contrast to liquid-filled zones, presumably due to the variations in density caused by the "working" of gas in the drilling fluid at or near the borehole. It should be recognized that this characteristic may be diagnostically used to advantage in certain instances.

The Sonic Log

The introduction of the sonic log improved porosity determinations in the Permian carbonates. First impressions by interpreters accustomed to neutron log characteristics were, in many cases, pessimistic. This was often due to the somewhat compressed response of the sonic log relative to the neutron because of the presence of evaporites. The effect of gypsum is to expand the neutron survey to indicate higher porosities compared with the sonic log. In an anhydritic zone of low porosity, however, the sonic log will indicate a slightly high apparent porosity when average dolomite or limestone matrix data are used. This is due to the relatively lower velocity of sound through anhydrite. The result is to reduce the over-

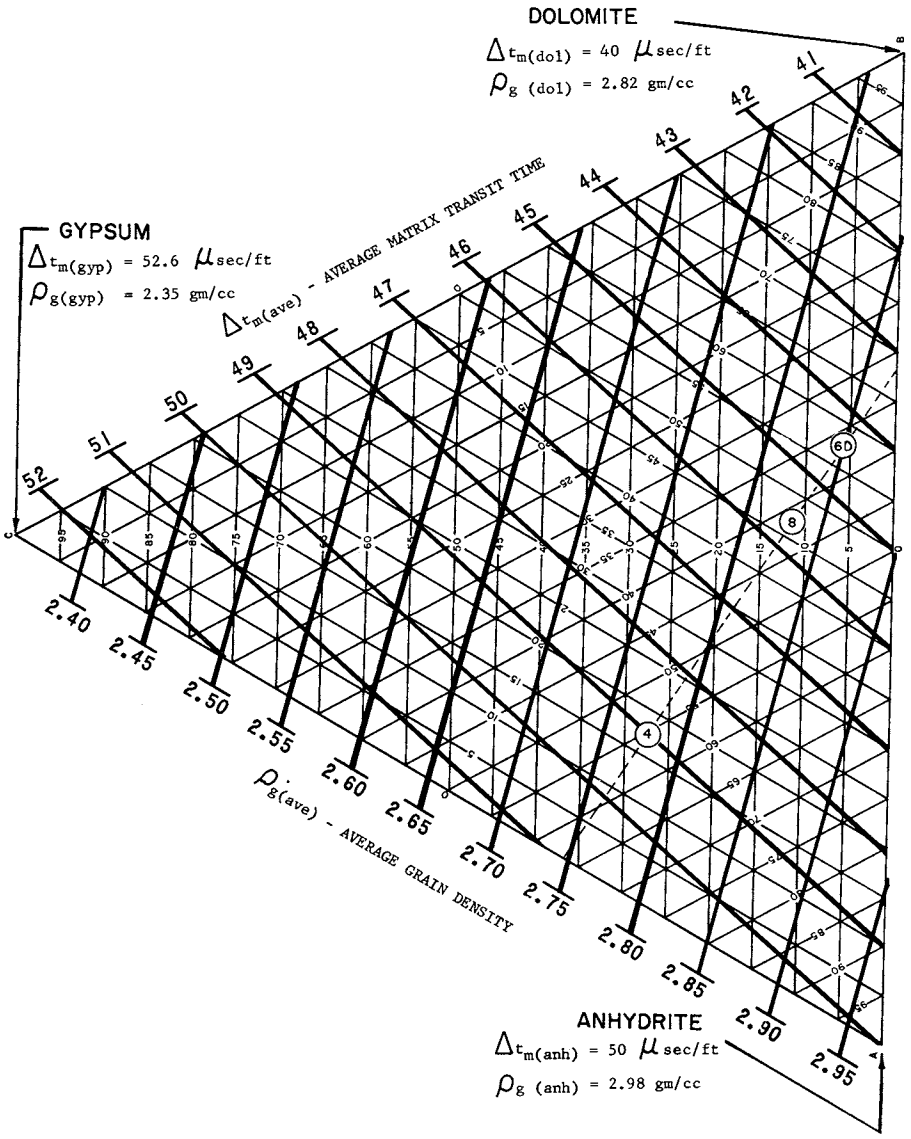

Fig. 6—Triangular co-ordinate graph.

all sonic log deflection and de-emphasize certain of the characteristics which were so apparent on the neutron survey.

Practical use in the field has demanded the application of average matrix data. Graphic comparisons of sonic transit time read from the surveys and porosity information derived from core analysis serve as a basis for commonly used matrix velocities. Because the velocities of gypsum (approximately 19,000 ft/sec)[8] and anhydrite (20,000 ft/sec) are somewhat less than that of the dolomite (25,000 ft/sec) or limestone (23,000 ft/sec), the average matrix velocities derived by this method will of necessity be somewhat low, usually in the range of 22,500 ft/sec to 23,000 ft/sec. In practice, however, it becomes apparent that certain horizons indicate porosities less than zero using these averages. This points out that some of the carbonates, in this case lacking evaporites, must possess matrix velocities in a range of 25,000 ft/sec or higher. One source[9] indicates 26,000 ft/sec as the apparent matrix velocity of dolomite.

The commonly accepted inability of the sonic log to accurately evaluate non-uniform porosity distribution in fractured and vugular carbonate rocks remains an obstacle to general interpretation. We may allay some of our fears, however, in that somewhat regular, distributed, solution and intercrystalline porosity is often present in Permian dolomites, and many fractures are either partially or completely filled. This, in most cases, permits the use of the Wyllie time-average equation. Porous rocks containing little or no matrix porosity must, for a time, present a sonic interpretation problem, although some acoustic methods may at present indicate qualitatively the presence of the condition.

Whatever the problems that have been encountered, the time-average equation continues to be useful. When the matrix composition of an evaporitic carbonate is considered, the sonic response may be expressed by:

$$\Delta t = \phi \Delta t_f + (1 - \phi)\Delta t_{m(ave)} \quad (4)$$

where

$$\Delta t_{m(ave)} = D\Delta t_{m(dol)} + A\Delta t_{m(anh)} + G\Delta t_{m(gyp)} \quad . \quad . \quad . \quad (5)$$

Δt = the average sonic transit time (micro-sec/ft) read from the log

Δt_f = the sonic transit time through the interstitial fluid

$\Delta t_{m(ave)}$ = the average matrix transit time from the Wyllie time-average equation

$\Delta t_{m(dol)}$ = 40.0 micro-sec/ft, the sonic transit time through dolomite

$\Delta t_{m(anh)}$ = 50.0 micro-sec/ft, the sonic transit time through anhydrite

$\Delta t_{m(gyp)}$ = 52.6 micro-sec/ft, the sonic transit time through gypsum

ϕ = the porosity.

D, A and G are the respective fractions of matrix of each mineral as shown in the density relationship and $D + A + G = 1$.

When the matrix is comprised of limestone, anhydrite and gypsum, Eq. 5 is appropriately altered and a $\Delta t_{m(lime)}$ of 43.5 micro-sec/ft is used.

It is of interest to note that a dense anhydrite zone with no porosity will indicate an apparent porosity of 3.8 per cent if an average matrix velocity of 22,500 ft/sec is utilized. A similar gypsum zone would indicate an apparent porosity of 5.7 per cent.

Sonic "skip cycling" or, in many cases, long transit times cannot reliably be considered gas zones in carbonate intervals without the benefit of additional information. The effects of fractures, or thin beds with markedly contrasting matrix velocities, may produce these phenomena. Such zones remain, however, highly suspect.

Theoretical Considerations

Because the neutron, sonic and density logs give independent solutions to porosity and range of matrix composition, it should be possible to solve for these values repeatedly, and eventually find a solution for which all logs would be in agreement. If this were accomplished, not only a more accurate porosity value would be obtained for use in computing oil in place, but variation in the gen-

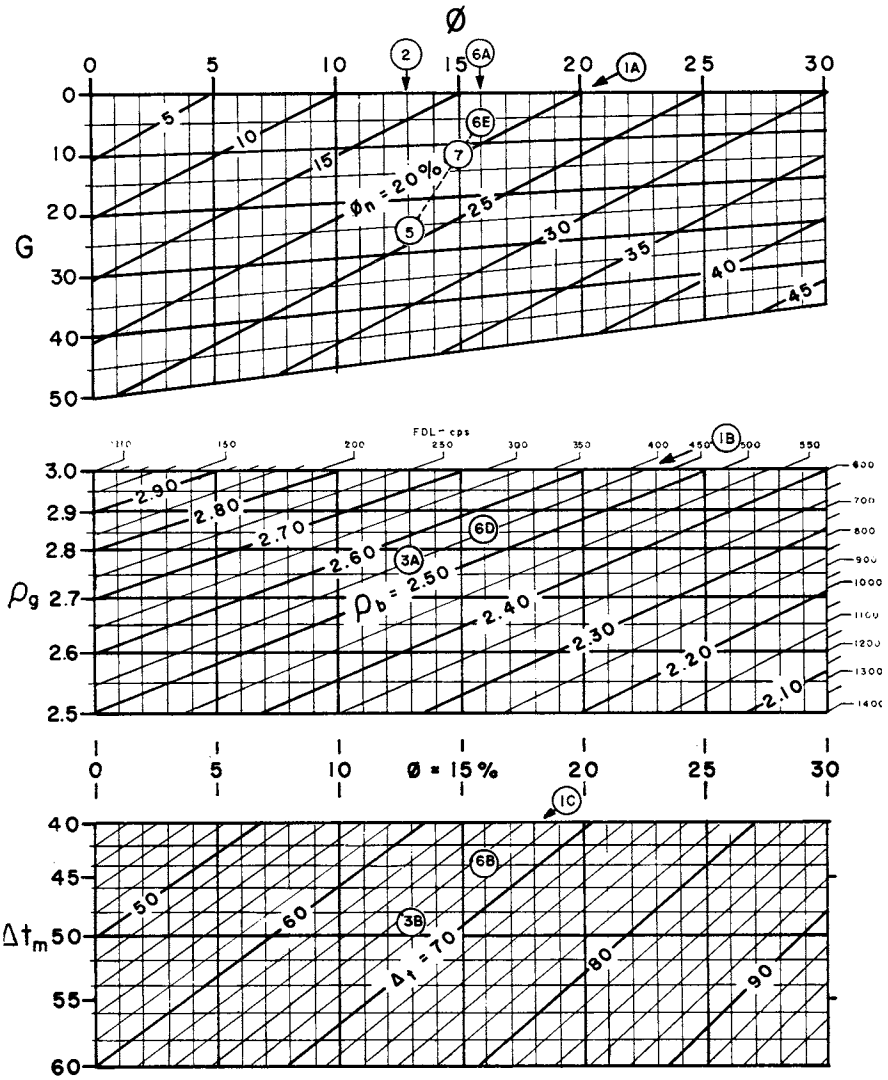

Fig. 7—Uniform porosity scale which combines solutions to Eqs. 1, 2 and 4.

erally known rock composition could be described quantitatively.

The iterative solution suggested above may be shortened by employing a graphical procedure. Figs. 6 and 7 illustrate this type of solution. The triangular coordinate graph (Fig. 6) gives all possible solutions to the equations:

$$\rho_{m(\text{ave})} = D\rho_{g(\text{dol})} + A\rho_{g(\text{anh})} + G\rho_{g(\text{gyp})} \quad . \quad . \quad . \quad (3)$$

$$\Delta t_{m(\text{ave})} = D\Delta t_{m(\text{dol})} + A\Delta t_{m(\text{anh})} + G\Delta t_{m(\text{gyp})} \quad . \quad . \quad . \quad (5)$$

For these three minerals, it is readily seen that any particular combination gives a unique solution for both $\Delta t_{m(\text{ave})}$ and $\rho_{m(\text{ave})}$.

Fig. 7 combines, on a uniform porosity scale, solutions to the following three equations:

$$\phi_n = \phi + (1 - \phi)\,(0.49G) \quad . \quad (1)$$

$$\rho_b = \phi\,\rho_f + (1 - \phi)\,\rho_{m(\text{ave})} \quad . \quad (2)$$

$$\Delta t = \phi\Delta t_f + (1 - \phi)\,\Delta t_{m(\text{ave})} . \quad (4)$$

For the sample computation illustrated, the following data are given by logs: Δt: 67 micro-seconds/ft, density log: 410 cps, neutron ϕ: 20 per cent. For this example we find: $\phi = 15$ per cent, $D = 47$ per cent, $A = 41$ per cent, $G = 12$ per cent, $\Delta t_{m(\text{ave})} = 45.6$ micro-seconds/ft, $\rho_{g(\text{ave})} = 2.83$ gm/cc.*

The author feels that the graphical solution offers the advantages of good visualization of the problem, plus easy adaptation for new mineral systems, since only the triangular graph need be modified for different matrix minerals.

A direct solution to the problem is possible by expansion of Eqs. 1, 4 and 2 to the form:

$$\phi_n = \phi + 0.49G' \quad . \quad . \quad . \quad . \quad (1A)$$

$$\Delta t = \phi\Delta t_f + D'\,\Delta t_{m(\text{dol})} + A'\Delta t_{m(\text{anh})} + G'\Delta t_{m(\text{gyp})} \quad . \quad . \quad . \quad . \quad . \quad . \quad . \quad . \quad . \quad (4A)$$

$$\rho_b = \phi\rho_f + D'\,\rho_{g(\text{dol})} + A'\rho_{g(\text{anh})} + G'\rho_{g(\text{gyp})} \quad . \quad . \quad . \quad . \quad . \quad . \quad . \quad . \quad (2A)$$

To use these expressions, re-definition of the symbols D, A and G is necessary. These symbols were previously defined as fractions of matrix composition. D', A' and G' are defined as fractions of bulk volume. From this definition, a fourth formula may be written:

$$1 = \phi + D' + A' + G'.$$

This produces four equations with four unknowns which are amenable to quick and easy solutions by electronic computers. Fig. 8 shows the results of a machine solution of these simultaneous equations in a San Andres well in Crane County. The printer has been programmed to give an analog output so that it is necessary only to connect the printed characters to produce this illustration.

A nomograph has also been constructed to effect the same solution. Figs. 9 and 10 show this nomographic procedure, using the following parameters:

Fluid Δt_f — 188.7 micro-sec/ft ρ_f 1.0 gm/cc

Dolomite Δt_m — 40.0 micro-sec/ft ρ_g 2.82 gm/cc

Anhydrite Δt_m — 50.0 micro-sec/ft ρ_g 2.98 gm/cc

Gypsum Δt_m — 52.6 micro-sec/ft ρ_g 2.35 gm/cc.

For the sample computation on these figures, the log data from the graphical solution are used again. Fig. 9 is used to solve for porosity and G'. In cases where detailed lithology identification is not wanted and no gas problems exist, computation may stop here. If the additional data is required, Fig. 10 is entered with the log data plus porosity and G' to find D' and A'.

The solution from this sample data gives: porosity = 15 per cent, $D' = 40$ per cent, $A' = 35$ per cent and $G' = 10$ per cent.

It will be noted that D', A' and G' are respectively smaller than the values of D, A and G found graphically. The amount of this difference is shown by the formulas:

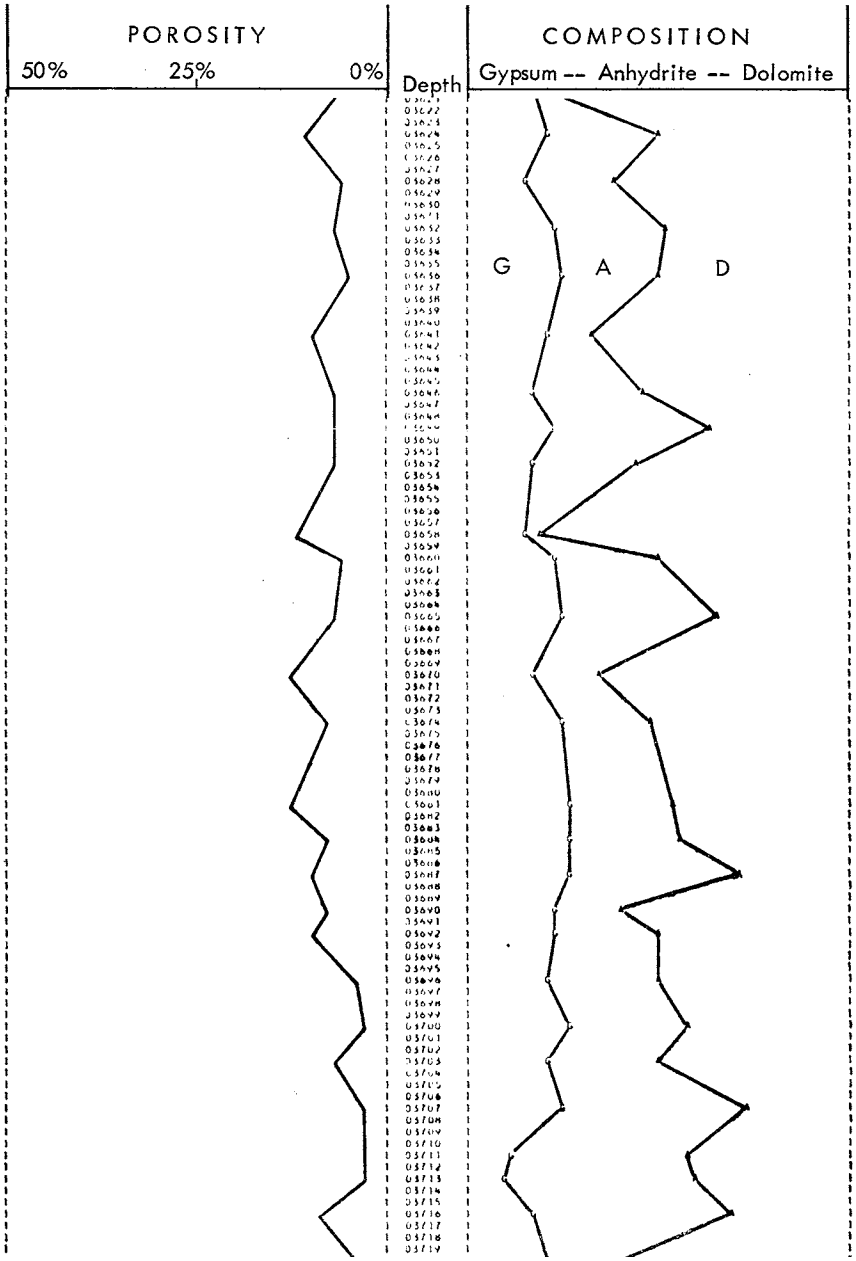

Fig. 8—A print-out of machine computed data.

*A detailed description of the graphical solution and of graph construction appears in the Appendix.

$$D = \frac{D'}{1 - \phi}$$

$$A = \frac{A'}{1 - \phi}$$

$$G = \frac{G'}{1 - \phi}$$

which expresses D, A and G as per cent of rock matrix rather than per cent of bulk volume. The use of either is a matter of personal preference. In this paper, forthcoming illustrations show composition as per cent of rock matrix and porosity values are shown separately for comparative purposes.

Interpretation and Results

The difficulties in verifying the composition data obtained by computation are many. To adequately sample a representative volume of rock investigated by the surveys approaches impossibility and is certainly impractical. Sampling of any kind can be expected to give only a qualitative comparison because of local lithologic heterogeneity. However, when a particular mass of rock, sufficiently thick to be resolved by each survey, becomes monomineralic or near so, the validity of certain data may be checked intuitively. For example, if the mineral is anhydrite, the individual surveys should respond with aforementioned characteristics. Fig. 11 illustrates such a case where a slightly porous anhydrite zone is well defined between impervious evaporitic dolomite intervals.

If only a sonic log were run through the zone illustrated in Fig. 11, and no specific knowledge of mineralogic changes were available, an average matrix velocity for dolomite of 22,500 ft/sec or 23,000 ft/sec might well be employed. A porosity of approximately 5.6 per cent would be indicated. If, for certain reasons, matrix velocities of 24,500 ft/sec or higher were used, a porosity of 7.8 per cent or greater would result. On the presumption that the zone might be anhydrite (20,000 ft/sec), the calculated porosity would be approximately 1.8 per cent.

If only a neutron log were run, an average nomographic solution would exhibit approximately 1.2 per cent porosity. If only a density log were run, the indicated bulk density of 2.95 would reflect a porosity of 1.7 per cent, if the zone were presumed to be anhydrite by observation of the high bulk density.

It can be seen that there is very close correlation of the porosities when anhydrite parameters are considered, in spite of the fact that the exact composition is not known. In this particular instance, the density log is an excellent guide because the indicated bulk density is well above the matrix densities of the expected composition and approaches the grain density of anhydrite.

If all three surveys are run, a solution satisfying the response of all logs resolves these slight differences to a common porosity of 1.5 per cent and defines the composition to fit all equations indicating 100 per cent anhydrite, 0 per cent dolomite, and 0 per cent gypsum.

Observations of sufficiently large zones of gypsum which would allow

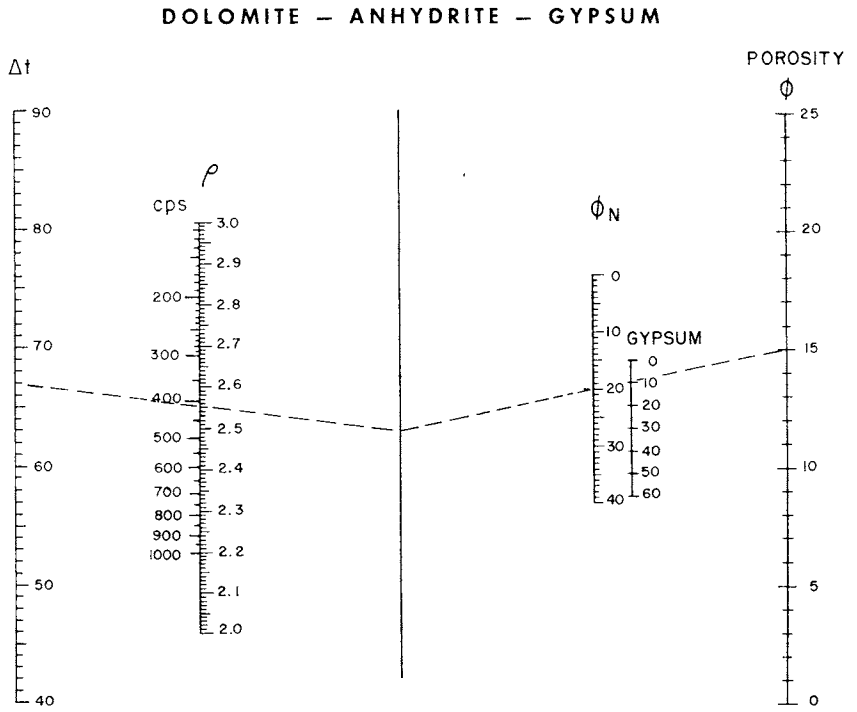

Fig. 9—Nomograph used to solve for porosity and G′.

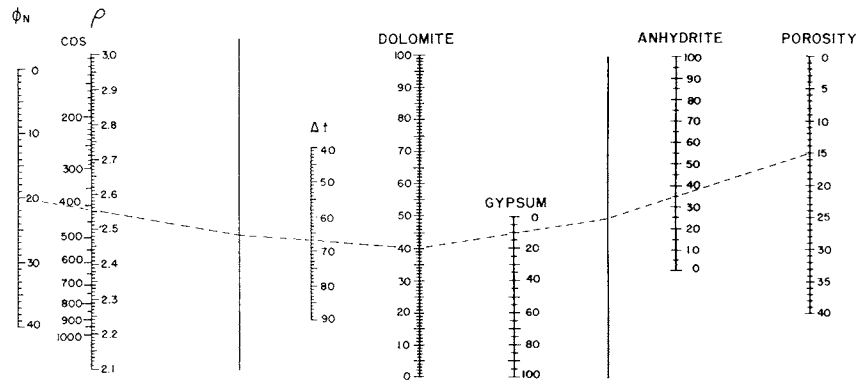

Fig. 10—Nomograph used to solve for D′ and A′.

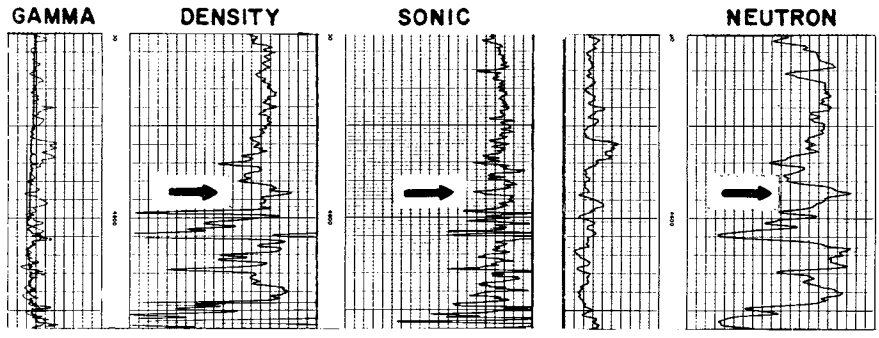

Fig. 11—A Clearfork well in Crane County, Tex.

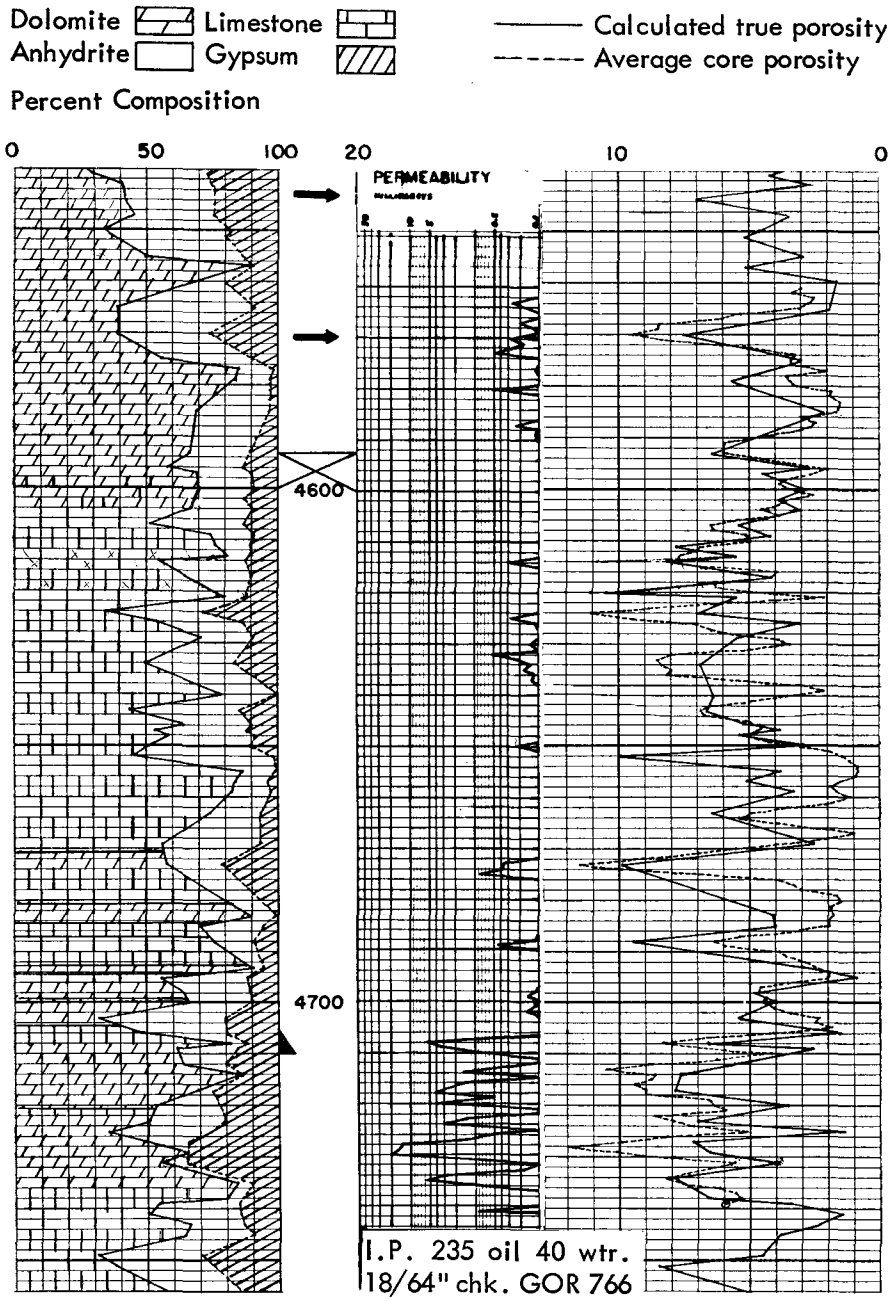

Fig. 12—A Clearfork well in Crane County, Tex. True porosity is shown compared to a running 3-ft average of porosities obtained from gypsum-free core analysis. Compared matrix composition is indicated on the left. The permeable interval at the bottom of the section produced salt water after stimulation. The arrows indicate the productive horizons in which the well was completed.

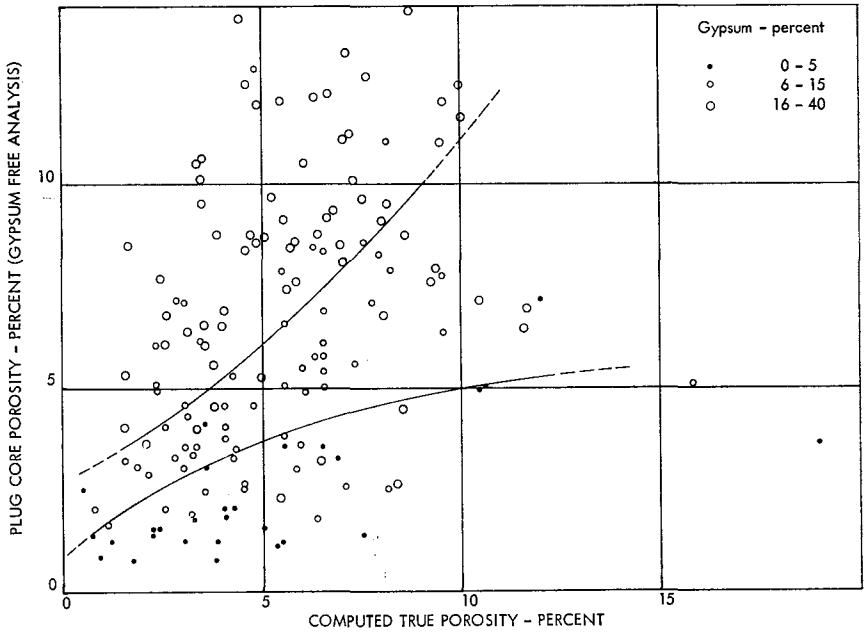

Fig. 13—Quantitative variations in porosities.

calculation of limiting parameters at the low end of the density spectrum are conspicuously lacking in our investigations to date.

Interesting situations, however, have been noted in cored intervals described as dense, blue-white anhydrite with indications of earthy white gypsum and irregular dolomite nodules. In two cases where bed thickness is indicated as 2 and 3 ft, the observed parameters and calculated results are shown in Table 1.

The apparent neutron (ϕ_n) porosity and true porosity (ϕ) are interesting contrasts. It is encouraging that the computations indicate the presence of dolomite in quantities which appear to correspond reasonably with that observed in the cores.

A comparison of porosities derived by computation and by "gypsum-free" core analysis in which precautions were taken to avoid gypsum effects is shown in Fig. 12. The core porosities are also shown as running 3-ft averages to better match the investigation of the logging tools. The calculated composition is shown on the left side of the log. The changes from limestone to dolomite were indicated by examination of the cores. Qualitative changes in porosity correlate well, but show interesting quantitative variations. Fig. 13 illustrates these variations by grouping the porosities according to the amount of calculated gypsum present. The intervals with small amounts of gypsum (0-5 per cent) are limited, with few exceptions, to low porosities. The log in Fig. 12 shows these zones to possess very little permeability and the gypsum is accompanied by relatively low computed values of anhydrite. Intervals which

contain 6 per cent to 20 per cent gypsum indicate somewhat regular distribution about a line with a slope of one. Those intervals containing more than 20 per cent gypsum indicate consistently higher porosities from core analysis than from computation.

An obvious presumption at this stage might be that low porosities are more accurately measured by logging methods. The small amount of gypsum present, in this case, can contribute little apparent porosity even though there may be a tendency toward some dehydration. A more important factor, however, is that accurate porosity values measured by Boyles Law expansion porosimeter are difficult, if not impossible, to obtain in these low porosity ranges where there may be only a trace of permeability.

It would appear, throughout a wide range of porosities, that gypsum has experienced some dehydration in routine laboratory work, accounting for generally higher core porosities when gypsum is indicated to be present in quantities above 20 per cent.

The computed log of a dolomite section containing large amounts of gypsum is shown in Fig. 14. The right side of the log compares apparent neutron porosity and calculated true porosity. This well is in an area of pumping wells, the past productivity of which does not correlate with the indicated neutron porosities. Single point entry and stimulation at the points indicated produced a flowing oil well with an initial potential of 201 BOPD and 22 bbl water with a gas-oil ratio of 1,550:1. Occurrences of this type, exhibiting generally low true porosities and relatively high fractions of gypsum, have shown apparently unreasonable differences in the appearance of water from well to well, and mark the transition to poor or nonproductive horizons nearby.

It has been found, in many cases where gas is present, that a solution for porosity and composition cannot be obtained. This is indicated in the graphical method by values which fall outside the triangular composition grid. Machine computation will force a solution and provide data which is easily recognized as imaginary. A readout may be provided which, when this situation is encountered, indicates gas.

Within carbonate sections, scattered gas indications which are seemingly out of place may be due to errors in digitized information, unpredicted changes in rock mineralogy, or to the presence of gas. Certain mineralogical changes can be detected by using the gamma-ray log as a guide, whereupon corrections may be considered or the points omitted. If no resolution or reading error is detected, the presence of gas must be considered.

The effect of gas upon the density, neutron and sonic logs is well known. A deterent to the use of these logs for the express purpose of locating gas is the unpredictable nature of liquid invasion. However, if invasion is shallow or gas movement persists in the immediate vicinity of the borehole, good results should be obtained.

TABLE 1

ρ_b	Δt	ϕ_n (Per Cent)	ρ_g	$\Delta t_{m\,(ave)}$	ϕ (Per Cent)	Anh. (Per Cent)	Gyp. (Per Cent)	Dol. (Per Cent)
2.69	50	18.8	2.709	48.4	1.1	38.5	36.5	25
2.68	51	15.25	2.745	46.5	4.0	22.5	23.5	54

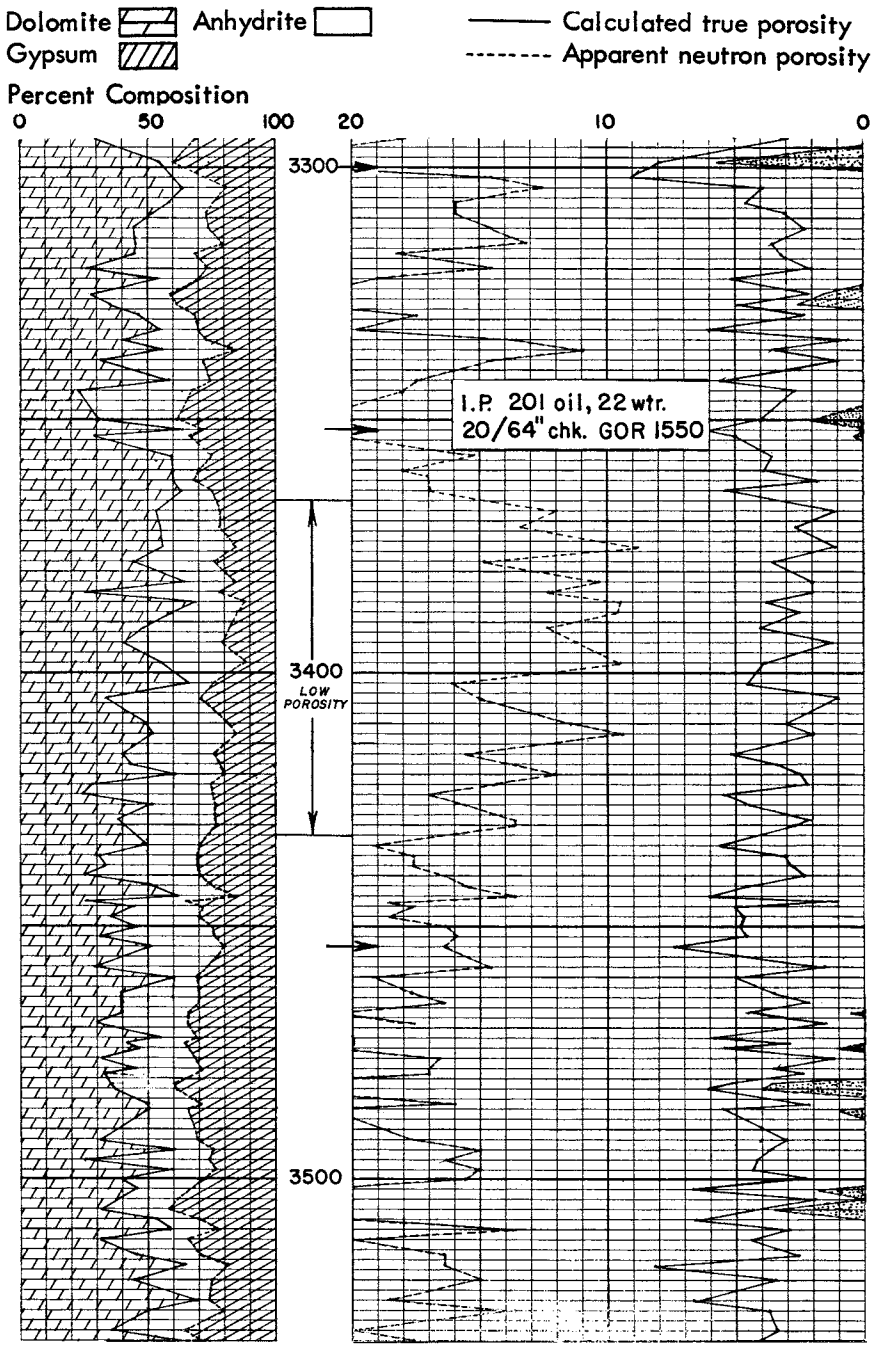

Fig. 14—A San Andres well in Crane County, Tex. Apparent neutron porosity and calculated true porosity are compared on the right. Points of entry (indicated by arrows) produced the fluid indicated above after treatment. The relatively large percentages of gypsum and generally low true porosities appear to mark the transition to lateral reservoir boundaries.

The calculated porosity log shown in Fig. 15 indicates the presence of gas in the upper and lower part of the illustrated section. The upper gas interval is associated with an oil column. The latter occupies the center of the section where plotted porosity indications are continuous. The gas indicated in the lower one third of the section is a separate reservoir isolated from above by a zone of low porosity. A production test at the base of the zone flowed 1.4 Mcf/D of gas, and thus confirmed the indications of the computed log.

The accompanying logs in Fig. 15 are included to show the porosities indicated by each as a result of using average matrix data. Apparent porosities from surveys designated are compared with computed true porosities. Consecutive omissions from the true porosity curve indicate the presence of gas. The base of the gas zone (below 4,570 ft) was production tested through perforations at 4,754 ft and flowed 1.4 Mcf gas/D. The well was completed in the oil reservoir (perforated at 4,456 ft). The gas-oil ratio was slightly high because of the proximity of the upper gas cap.

The density and neutron logs are currently being used in a number of different lithologies for the detection of gas, without the benefit of the sonic log. It should be mentioned that a gypsiferous or an argillaceous zone may effect a somewhat high neutron response which may obscure the gas indication sought.

Density log porosities, derived from average matrix data, are compared to neutron porosities in Fig. 17. The true porosity log shown in the same figure delineates a gas horizon. Apparent neutron porosities within the gas interval are higher than those shown by the density log, reflecting gypsum in the formation, in this case as high as 29 per cent. The effects of gypsum, however, are detected by the use of the sonic log, which permits resolution of the gas zone. A nearby well corroborates the presence of gas in the interval shown.

Certain points throughout calculated gas zones permit a solution for composition and porosity. This is considered to be a realistic condition in that some beds of very low permeability may not be gas bearing, particularly those in the low porosity ranges.

Figs. 16 and 18 show the comparative response of the density, neutron and sonic logs as recorded in the wells which are interpreted in Figs. 15 and 17, respectively.

Snap judgments on the basis of cursory, visual examination of only the well logs are discouraged. Samples or cores should be consulted to determine the variations in lithology. This becomes especially important if a detailed reservoir study is to be undertaken where both limestone and dolomite facies are present. The entire section should be studied based on the computed results of all three logs. Fig. 19 shows the density, neutron, and sonic logs of a short section equivalent to that which indicated gas throughout in Fig. 15, at approximately the same subsea datum. The density log exhibits a low bulk density, and would suggest the presence of gas. Calculations would, in fact, show the zone to be gas if the interval were considered to be dolomite instead of limestone. By the use of data from all three logs, however, this zone is shown to be much less anhydritic than the adjacent intervals, while containing approximately the same amount of gypsum. Porosity is 9 per cent. Single point entry and stimulation resulted in 19 BOPD with a gas-oil ratio of 1,563:1 from this interval. Porosity at the bottom of the section tested only salt water and a small amount of gas.

The importance of knowing that certain horizons lack porosity and possessing some knowledge of the reason why is as important as knowing where and how much porosity is present. The ability to differentiate evaporitic horizons in terms of anhydrite and gypsum and to delineate intervals which play an important role in the entrapment or guidance of hydrocarbons, either during the original accumulation or the productive life of a reservoir, may lead to new productive horizons. Such information can delineate closely superimposed reservoirs in similar lithologies and may serve as a guide to more efficient completion techniques.

Conclusions

Considerable lithologic variation occurs in Permian carbonate rocks; and gypsum and anhydrite are common constituents. The effect of gypsum is to produce optimistic poros-

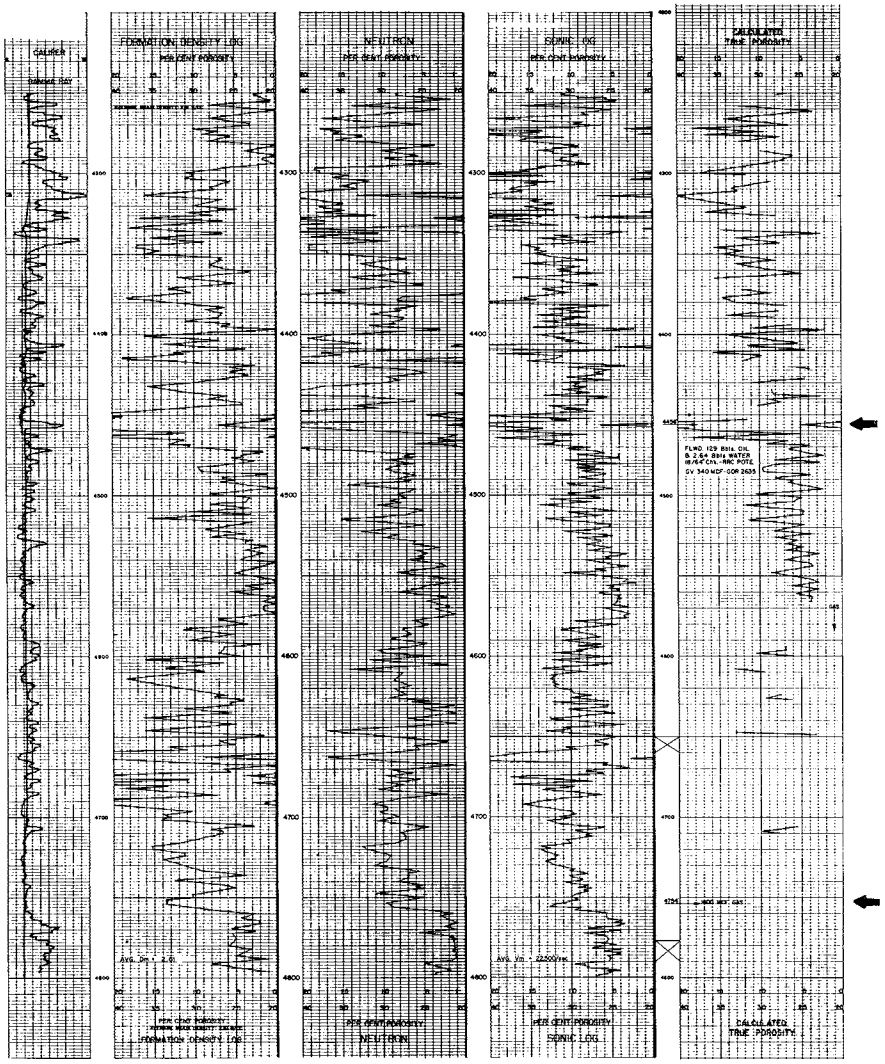

Fig. 15—A Clearfork well in Crane County, Tex.

ities in core analysis and in the interpretation of neutron logs.

The innovation of improved sonic and density logs has provided other information reflecting diagnostic rock characteristics. The presented system of interpretation produces more reliable porosity determinations in complex carbonate lithologies by the simultaneous solution of data from three independent porosity devices.

Using mineral matrix information, effective reservoir boundaries can be defined.

The quantitative approach to the determination of lithology provides information which can aid in delineating the stratigraphic reservoir and assist in the recognition of water-bearing horizons and impending reservoir limits.

Where conditions permit, the ability to detect gas may be used to advantage.

It remains to extend the practical use of similar methods to other lithologies and to apply obtained information to reservoir or regional facies studies.

Nomenclature

ρ_b = Bulk density, obtained from the formation density log, gm/cc

ρ_f = Density of the interstital fluid, gm/cc

$\rho_{g(ave)}$ = Average grain density of the matrix, gm/cc

$\rho_{g(dol)}$ = Grain density of the dolomite, gm/cc

$\rho_{g(anh)}$ = Grain density of the anhydrite, gm/cc

$\rho_{g(gyp)}$ = Grain density of the gypsum, gm/cc

Δt = Average transit time of the formation, obtained from the sonic log, micro-sec/ft

Δt_f = Transit time of the interstitial fluid, micro-sec/ft

$\Delta t_{m(ave)}$ = Average transit time of the matrix, micro-sec/ft

$\Delta t_{m(dol)}$ = Transit time of the dolomite, micro-sec/ft

$\Delta t_{m(anh)}$ = Transit time of the anhydrite, micro-sec/ft

$\Delta t_{m(gyp)}$ = Transit time of the gypsum, micro-sec/ft

ϕ = Calculated true porosity of the formation

ϕ_n = Apparent porosity, or hydrogen index derived from the neutron

D = Calculated fraction of dolomite, or dolomite index, fraction of the rock matrix

A = Calculated fraction of anhydrite, or anhydrite index, fraction of the rock matrix

G = Calculated fraction of gypsum, or gypsum index, fraction of the rock matrix

D' = Calculated fraction of dolomite, or dolomite index, fraction of the bulk volume

A' = Calculated fraction of anhydrite, or anhydrite index, fraction of the bulk volume

G' = Calculated fraction of gypsum, or gypsum index, fraction of the bulk volume

Acknowledgments

The author wishes to express his appreciation to the management of Gulf Oil Corp. for permission to publish this paper, and to Jack Burke with Schlumberger Well Surveying Corp., who has taken an active part in the preparation of the paper and whose personal interest and work in computer programming has accelerated the practical use of the ideas herein expressed.

References

1. Towle, G. H.: "An Analysis of the Formation Factor—Porosity Relationship of Some Assumed Pore Geometrics", Third Annual Logging Symposium, Society of Professional Well Log Analysts (1962).
2. Waldschmidt, W. A. *et al.:* "Classification of Porosity and Fractures in Reservoir Rocks", *Bull.* AAPG (1956) **10,** No. 5, 953.
3. Goodman, N. R.: "Gypsum and Anhydrite in Nova Scotia", *Memoir No. 1,* Province of Nova Scotia Dept. of Mines (1952).
4. Bynum, R. S., Jr. and Koepf, E. H.: "Whole Core Analysis Methods and Interpretation of Data from Carbonate Reservoirs", *Jour. Pet. Tech.* (Nov., 1957) **IX,** No. 11, 11.

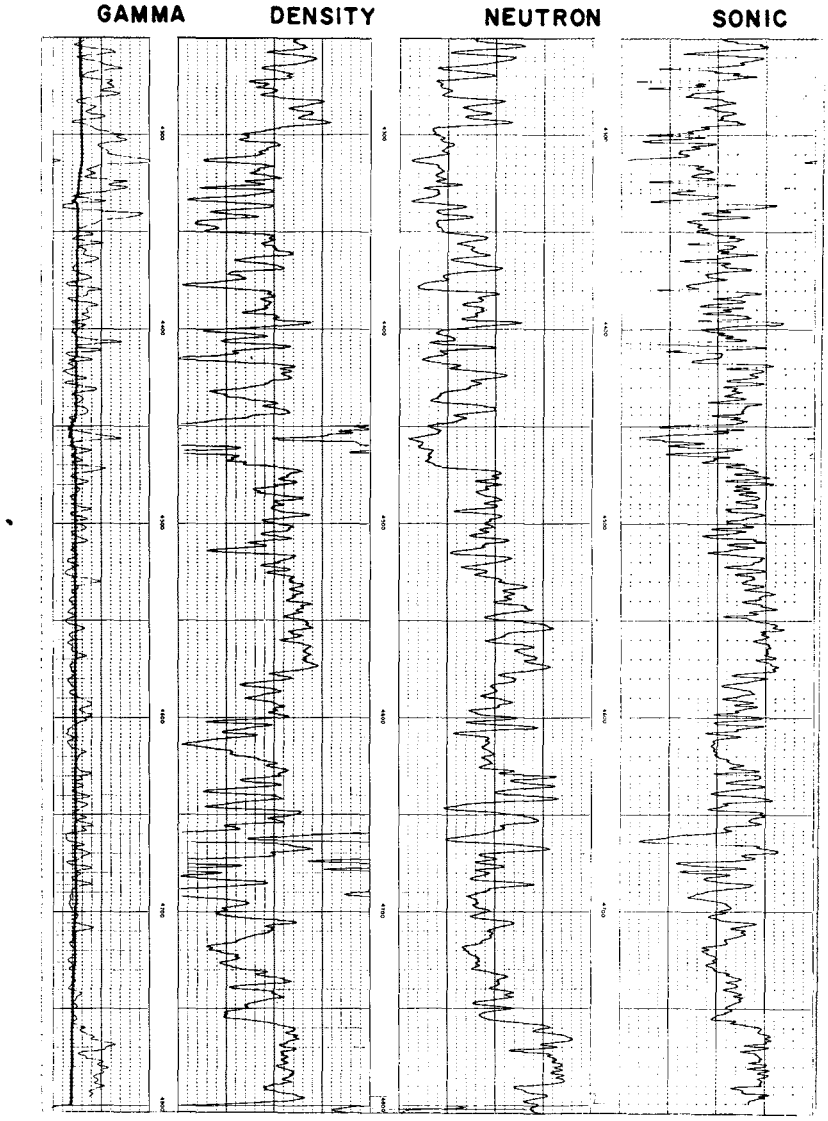

Fig. 16—The well logs from which Fig. 15 was derived are shown above for comparative purposes.

5. Hurd, B. G. and Fitch, J. L.: "The Effect of Gypsum on Core Analysis Results", *Jour. Pet. Tech.* (Sept., 1959) **XI**, No. 9, 221.
6. Lindley, R. H.: "The Use of Differential Sonic-Resistivity Plots to Find Movable Oil in Permian Formations", *Jour. Pet. Tech.* (Aug., 1961) 749.
7. Alger, R. P. *et al.*: "Formation Density Log Applications in Liquid Filled Holes", *Jour. Pet. Tech.* (March, 1963) 3.
8. Wyllie, M. R. J., Gregory, A. R. and Gardner, L. W.: "Elastic Wave Velocities in Heterogeneous and Porous Media", *Geophysics* (Jan., 1956) **XXI**, No. 1, 45.
9. Wyllie, M. R. J.: *The Fundamentals of Electric Log Interpretation*, 2nd Ed., Academic Press, Inc., New York (1957).

APPENDIX

Development of Graphs

The porosity graphs of Fig. 7 are solutions to the following equations:

$$\phi_n = \phi + (1 - \phi)(0.49G) \quad . \quad (1)$$

$$\rho_b = \phi\rho_f + (1 - \phi)\rho_{g(\text{ave})} \quad . \quad (2)$$

$$\Delta t = \phi\Delta t_f + (1 - \phi)\Delta t_{m(\text{ave})} . \quad (4)$$

The graphs were arranged to produce equivalent porosity values on the vertical lines for convenience in comparing the responses of the three logs. The log data (ϕ_n, ρ_b or *FDL* cps, and Δt) are entered on the diagonals and the matrix parameters (G, $\rho_{g(\text{ave})}$ and $\Delta t_{m(\text{ave})}$) are given on the horizontal lines.

The triangular graph of Fig. 6 consists of a base grid which solves the equation

$$1 = D + A + G.$$

The corners of the triangle represent 100 per cent of each mineral, and the numbers extending from each corner define constant percentage lines for that particular mineral. Any point within the triangle forms the intersection for three lines which give the percentage of each mineral for that point.

The base grid is overlain by two sets of parallel lines which are respective solutions for the following equations:

$$\rho_{g(\text{ave})} = D\rho_{g(\text{dol})} + A\rho_{g(\text{anh})} + G\rho_{g(\text{gyp})} \quad . \quad . \quad . \quad . \quad (3)$$

$$\Delta t_{m(\text{ave})} = D\Delta t_{m(\text{dol})} + A\Delta t_{m(\text{anh})} + G\Delta t_{m(\text{gyp})} \quad . \quad . \quad . \quad (5)$$

The construction of these lines is simple, making modifications of this graph for new mineral combinations quick and easy.

It may be readily seen that linear division of each side of the triangle between the values given at the corners produces the values shown.

It remains only to connect points of equal transit time and matrix density to produce the lines of constant $\Delta t_{m(\text{ave})}$ and $\rho_{g(\text{ave})}$ as shown.

Method of Solution

The iterative computation may be made with no more than two trial solutions by a method which is best shown by working an example.

The following values are given from the logs: $\phi_n = 20$ per cent, density log = 410 cps, sonic log = 67 micro-sec/ft. The solution is made as follows:

1. Draw lines, paralleling the diagonals, for ϕ_n (1*A*), density cps (1*B*), and Δt (1*C*).

2. Draw a line for any value of porosity (in this case 13 per cent) through all three graphs.

3. Find the values of $\rho_{g(\text{ave})}$ (3*A*) and $\Delta t_{m(\text{ave})}$ (3*B*) which correspond to this porosity ($\rho_{g(\text{ave})} = 2.78$, $\Delta t_{m(\text{ave})} = 49$).

4. On Fig. 6 place a point at the intersection of $\Delta t_{m(\text{ave})}$ (4) and $\rho_{g(\text{ave})}$ found in Step 3.

5. Read the value of G found above (27 per cent) and enter this value (5) in the top portion of Fig. 7 on the porosity line from Step 2. This procedure corresponds to solving all five equations for a particular value of porosity, and gives one possible solution for porosity. Agreement is shown if Point 5 falls directly on the ϕ_n diagonal.

6. If Point 5 falls below the ϕ_n diagonal, pick a higher value of ϕ (6*A*) and repeat Steps 2 through 5 for new

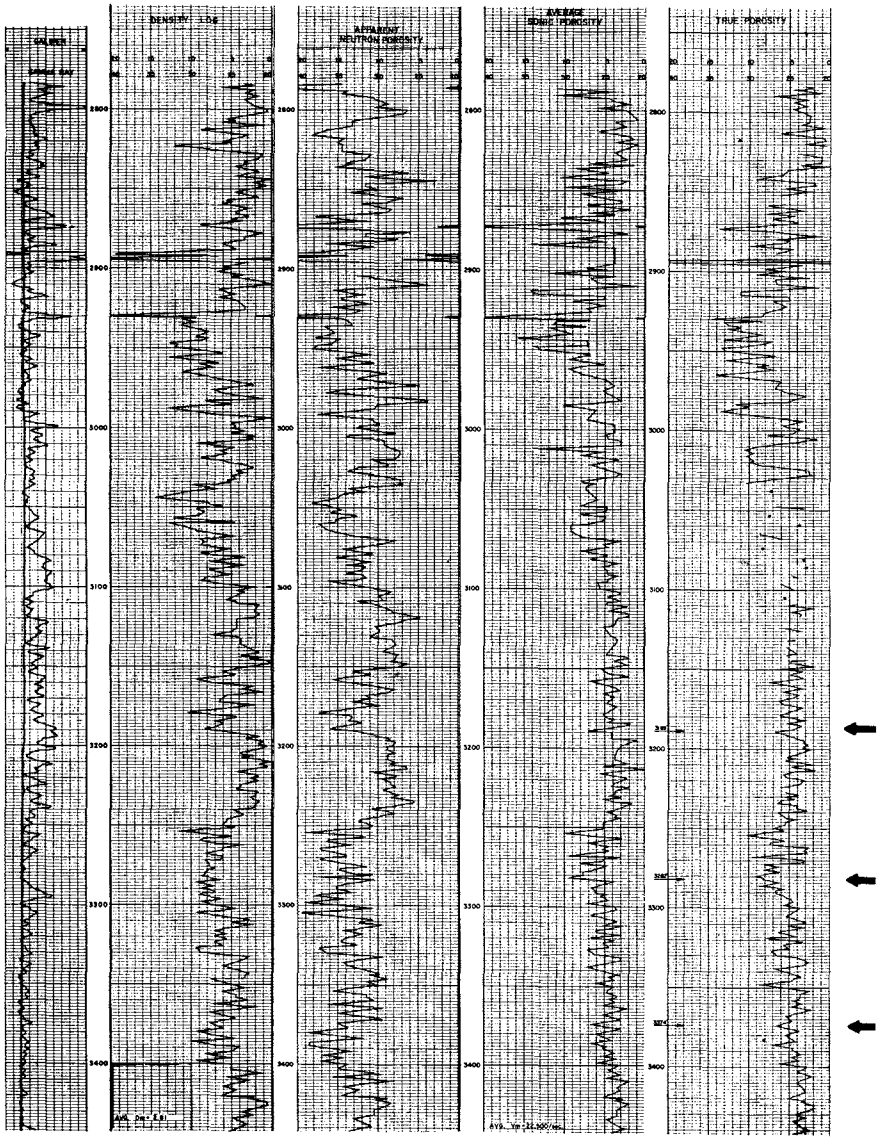

Fig. 17—Apparent porosities from surveys designated above are compared to computed true porosities. Consecutive omissions from the true-porosity curve indicate the presence of gas. The gas zone is corroborated by a production test in a nearby well, which recovered 1.3 MMcf/D of gas from a single-point entry at a point equivalent to 3,062 ft in this well. Recent tests, in nearby wells, of the upper 200 ft of this section have recovered little gas. This well was completed flowing 232.8 bbl of oil through a 24/64-in. choke with a gas-oil ratio of 816, from the perforations at 3,189, 3,282 and 3,374 ft.

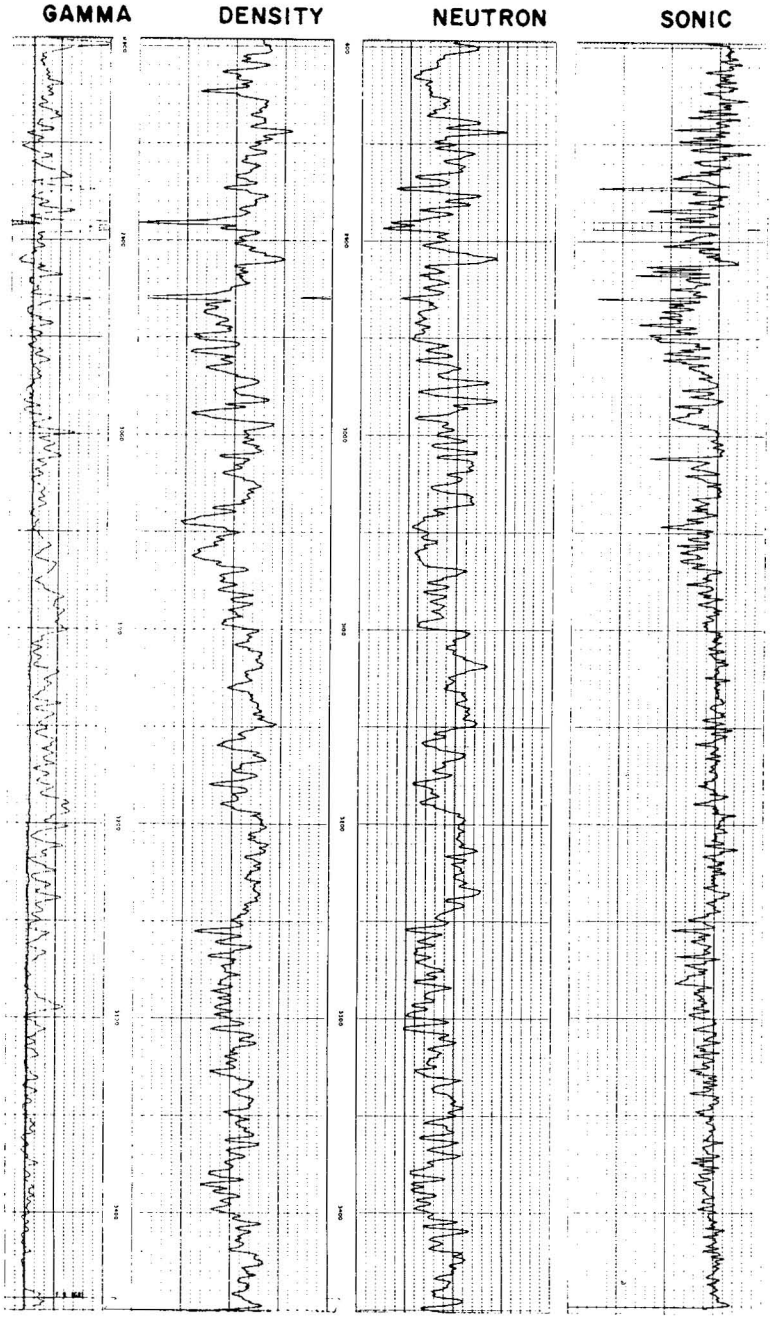

Fig. 18—A San Andres well in Crane County, Tex. The well logs from which the interpretation in Fig. 17 was derived are shown above for comparative purposes.

values of $\Delta t_{m(ave)}$ (6*B*), $\rho_{g(ave)}$ (6*C*), and G (6*D*). These steps result in the following values: ϕ = 16 per cent, $\Delta t_{m(ave)}$ = 44½ micro-sec/ft, $\rho_{g(ave)}$ = 2.85 gm/cc, G = 7 per cent. Conversely if Point 5 had been above the ϕ_n diagonal ϕ should be reduced.

7. Draw a line through Points 5 and 6*E*, on Fig. 7, to intersect the ϕ_n line. This intersection (7) is the only porosity which satisfies all three tool responses for porosity and matrix composition. (ϕ = 15 per cent, G = 12 per cent.)

8. Draw a line through Points 4 and 6*D* on Fig. 6 and place a point (8) on this line at the value of G found in Step 7. At this point the fractions of D and A can be read. (D = 47 per cent, A = 41 per cent.)

9. Should the point for Step 8 fall outside the triangular chart, solution is impossible for the parameters used.

The two major causes for impossible solutions are gas-bearing formations and the presence of minerals other than those included in the triangular graph. ★★★

WAYLAND C. SAVRE, *Sand Hills area geologist for Gulf Oil Corp. in West Texas, graduated from Iowa State U. with an MS degree in geology. He has been with Gulf since 1954 and has worked primarily with carbonate rocks and associated production problems as a reservoir geologist and log analyst.*

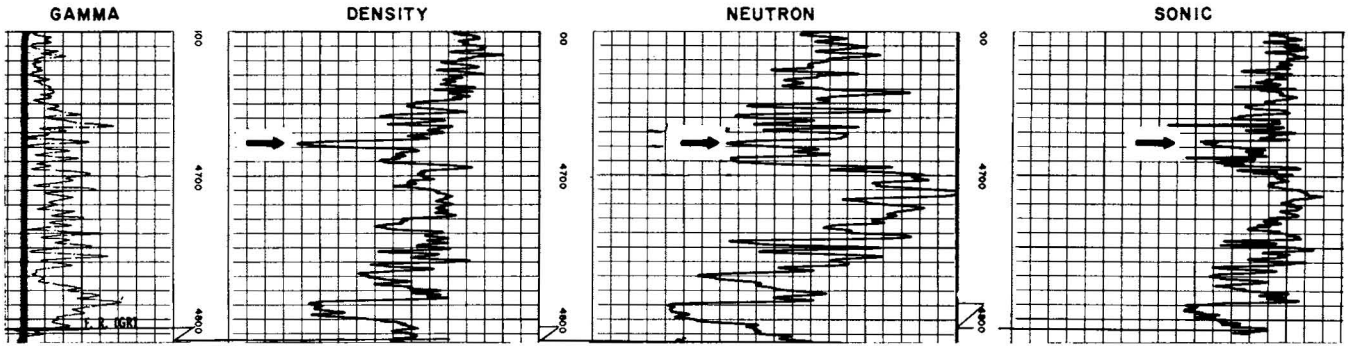

Fig. 19—A Clearfork well in Crane County, Tex. The Sonic and neutron logs show similar response to porosities throughout the interval shown. The density log exhibits a high relative deflection in the direction of higher porosity at 4,678 ft. Differences in response are indicated to be the result of composition changes rather than the presence of gas. The intervals above and below the point of interest indicate relatively larger amounts of anhydrite and lesser amounts of dolomite while the amount of gypsum throughout the entire zone varies only a small amount.